Journal of Photochemistry & Photobiology, A: Chemistry 446 (2024) 115138

Contents lists available at ScienceDirect

Journal of Photochemistry & Photobiology, A: Chemistry

journal homepage: www.elsevier.com/locate/jphotochem

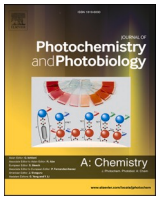

Reversal in solvatochromism, photochromism and thermochromism in a new bis-azo dye based on naphthalen-1-amine

İsa Sıdır [a,d,*], Yunus Emre Kara [b], Yadigar Gülseven Sıdır [a,d], Halil Berber [c], Rui Fausto [d,e]

[a] Department of Physics, Faculty of Science and Arts, Bitlis Eren University, 13000 Bitlis, Turkey
[b] Department of Physics, Sciences Institute, Bitlis Eren University, 13000 Bitlis, Turkey
[c] Department of Chemistry, Faculty of Science, Eskişehir Technical University, 26470 Eskişehir, Turkey
[d] CQC-IMS, Department of Chemistry, University of Coimbra, 3004-535 Coimbra, Portugal
[e] Istanbul Kultur University, Faculty Sciences and Letters, Department of Physics, 34158 Bakirkoy, Istanbul, Turkey

ARTICLE INFO

Keywords:
Azo dye
Reversal in solvatochromism
Photochromism
Thermochromism
Hydrogen bonding
Solvent effects

ABSTRACT

A novel bis-azo dye, 4,4′-((1*E*,1′*E*)-(oxybis(4,1-phenylene))bis(diazene-2,1-diyl))bis(naphthalen-1-amine) (abbreviated as **4odna**) was synthesized and characterized by IR and ^{1}H, ^{13}C and 2D COSY-NMR spectroscopies, and mass spectrometry. Optical properties were evaluated using UV–vis absorption spectroscopy. The observed solvatochromism was ascribed to the presence of different azo or/and hydrazone forms in solution. The azo forms show both positive and negative solvatochromism, with the reversal occurring for solvents with $E_T(30)$ ~45 kcal mol^{-1}, while the hydrazone tautomer shows negative solvatochromism. Application of the multiparametric Catalán and Kamlet-Taft linear solvation energy models allowed to evaluate the dependence of the solvatochromism exhibited by **4odna** on the hydrogen bond donating (HBD) and accepting (HBA) abilities of the solvent, as well as on their dipolarity (SdP) and polarizability (SP). Upon UV (λ = 311 nm) irradiation at room temperature, the compound was found to exhibit similar photochromic behavior in the polar-protic solvents methanol and ethanol, which is distinct from that observed in the polar-aprotic solvents dichloromethane, chloroform and chlorobenzene, with the hydrazone tautomer being photoconverted into the azo tautomer in the first group of solvents and vice-versa in the second group. In acetone, UV irradiation extensively transforms the compound into species with no absorption in the visible range, leading to fast discoloration of the solution. Temperature dependence of the color of the solutions of **4odna** in ethanol and chlorobenzene was also evaluated, and reversible thermochromic behavior was observed in the first solvent. In chlorobenzene, no thermochromism was observed, but a change of color of the solution was promptly induced by the UV–vis broadband source beam of the spectrometer when the absorbance spectrum of the solution was being recorded at T = 115 °C, which demonstrates that the azo forms of **4odna** undergo easy phototransformation into the hydrazone forms in this solvent at high temperature.

1. Introduction

Solvents may have significant influence on the mechanism, kinetics and thermodynamics of chemical processes [1–4]. These effects are commonly explained based on solvent properties like dipole moment, polarizability and hydrogen bond donor/acceptor capacity, which define the overall solvating ability of the solvent [1,4,5]. It is also well known that the solvent can strongly affect the spectroscopic properties of dyes, such as the wavelengths and intensities of the bands observed in their absorption and fluorescence electronic spectra [1–4].

The difference between the resolution energies of the initial and excited states differ in different solvents. This is manifested by changes in the spectral absorption profile, and as a result, the phenomenon in which the color of a solute varies in different solvents is called solvatochromism. Solvatochromism receives several applications, in particular in sensors, and in functional materials for construction of molecular switches. Solvatochromic compounds can also be used to measure solvent properties, which can then be used to explain solubility and predict suitable solvents for particular uses.

Sovatochromism can be interpreted using solvatochromic models, which rely on solvent polarity scales developed based on appropriate solvatochromic dyes [1–4,6,7]. The popular $E_T(30)$ solvent polarity

* Corresponding author at: Department of Physics, Faculty of Science and Arts, Bitlis Eren University, 13000 Bitlis, Turkey.
E-mail address: isidir@beu.edu.tr (İ. Sıdır).

https://doi.org/10.1016/j.jphotochem.2023.115138
Received 6 July 2023; Received in revised form 20 August 2023; Accepted 30 August 2023
Available online 3 September 2023

scale is based on the Reichardt's pyridinium *N*-phenolate betaine dye, 2,6-dipenyl-4-(2,4,6-triphenylpyridinium-1-yl)phenolate (this standard betaine dye had, by chance, the formula number **30** in the original manuscript, this fact justifying the use of the numeral **30** to refer to the dye [8]; E_T stands for electronic transition energy). This standard dye shows a strong negative solvatochromism (hypsochromic shift of the absorption maxima with the increase in the polarity of the solvent) as a result of its solvent-dependent HOMO → LUMO charge-transfer electronic absorption in the visible range (at about 850 nm, with $\varepsilon \approx$ 5000–7000 M^{-1} cm^{-1}) [1]. The Reichardt's $E_T(30)$ solvent polarity scale expresses the polarity of a given solvent in terms of the energy of the molar absorption energy (in kcal mol^{-1}) of the dye in that solvent, which can be determined using Eq. (1), where λ_{max} is the maximum of the band corresponding to the HOMO → LUMO charge-transfer electronic absorption of the dye, and *h*, *c* and N_A are Planck's constant, the speed of light, and Avogadro's constant, respectively. High $E_T(30)$ values correspond to a high solvent polarity, ranging from 63.1 kcal mol^{-1} for water to 30.7 kcal mol^{-1} for tetramethylsilane (TMS) [1].

$$E_T(30)\left(kcal\,mol^{-1}\right) = hcN_A/\lambda_{max} = 28591.5/(\lambda_{max}, nm) \quad (1)$$

Other dyes can be used to assess the polarity of the solvents using a similar approach and the same equation, where $E_T(30)$ is replaced by E_T(dye) [9,10].

Most frequently, dyes exhibit either single positive or negative solvatochromic behavior (corresponding to systematic bathochromic or hypsochromic shifts of the absorption maxima with the increase of the polarity of the solvent, respectively). Nevertheless, in some less frequent cases, a reversal in the solvatochromism is observed, in particular when moving from hydrogen bond acceptor to hydrogen bond donor solvents [11–13]. For example, Panigrahi and co-workers have reported on the reversal in the solvatochromism exhibit by a series of substituted benzylideneanilines and explained this property in terms of changes in the intramolecular hydrogen bonding pattern and conformational changes in the dyes [11], while de Melo et al. have reported on the reversal in the solvatochromism exhibited by azo dyes bearing dimethylamino electron-donor and nitro electron-acceptor groups in their structure [12]. For these compounds, the observed solvatochromism reversal was explained considering different contributions in different solvents of two resonance structures, a benzenoid form, which is better stabilized in less polar solvents and characterizes the region displaying positive solvatochromism, and a dipolar form, which is better stabilized in more polar solvents, in the region of negative solvatochromism [12]. Solvatochromism reversal has been recently reported as a novel strategy to develop more efficient activatable two-photon fluorescent probes for bioimaging [13].

Closely related with solvatochromism are solvent-dependent photochromism and thermochromism. The field of optoelectronics makes extensive use of organic compounds that demonstrate photochromism [14–20] and, among them, azo dyes have gained extensive attention due to their easy synthesis, high sensitivity and rapid response. Azobenzenes, for example, can undergo a reversible *trans–cis* photoisomerization under UV light [21–26], and have been suggested as candidates for applications such as photoswitching, information storage, nonlinear optics, and functional materials for use in biomedicine [27–35]. In recent years, the search for appropriate donor–acceptor substituents to tune the photoisomerization of azo dyes towards visible light has attracted widespread attention [29,36,37].

Following our previous recent investigation on the solvatochromism of 2-(*p*-tolyldiazenyl)naphthalene-1-amine (**2tona**), as well as on its photochromism and thermochromism in different solvents [7], in this article we describe the synthesis and characterization of a novel bis-azo dye, 4,4′-((1*E*,1′*E*)-(oxybis(4,1-phenylene))bis(diazene-2,1-diyl))bis(naphthalen-1-amine) (**4odna**), followed by the study of its solvato-, photo- and thermochromism. The compound's absorption spectra in solution of solvents with different characteristics were measured, and the observed color differences of the solutions were interpreted based on the solvent properties. The studied dye was found to exhibit reversal in solvatochromism with the change of solvent $E_T(30)$. The obtained solvatochromic data were also analyzed using the Kamlet-Taft and Catalán multiparametric empirical relations, in order to verify the contribution of the various solvent characteristics to the solvatochromism exhibited by the dye. Photochromism of **4odna** exposed to UV light with $\lambda = 311$ nm irradiation was also investigated in methanol, ethanol, acetone, dichloromethane, chloroform, and chlorobenzene solutions. In addition, **4odna** thermochromism studies were carried out in ethanol and chlorobenzene, within the 25–115 °C temperature range.

As it will be described in details in the next sections of this article, instrumental to the data analysis performed in this study is the consideration of azo-hydrazone tautomerism in the studied compound. This type of tautomerism has been found relevant to explain the solvatochromic properties of **2tona** [7], which share structural motifs with **4odna**, and has been addressed in detail for other azonaphthylamines and also for the structurally similar azonaphthols [38–44]. The optical properties of these compounds have been shown to be strongly influenced by solvents, in particular in the case of solvents exhibiting strong proton acceptor and/or proton donating abilities, since the azo-hydrazone tautomerism can be solvent mediated. Also, in some relevant cases, intramolecular proton transfer can be operative, if the molecules have the azo/hydrazone moiety located in the close vicinity of a proper group (as in *ortho*-hydroxyaryl Schiff bases) [45–47].

2. Materıals and Experımental methods

2.1. Synthesis

The synthesis of **4odna** was achieved in two steps (Scheme 1):

2.1.1. Step-1. Synthesis of diazonium salt

4.4′-Oxydianiline (1 mmol, 0.20 g) and $NaNO_2$ (11 mmol, 0.76 g) were weighed into a beaker, and 6 ml of cold distilled water were added to the mixture. The mixture was placed in an ice bath at a temperature between 0 and 5 °C. Six milliliters of cold distilled water and 6 ml of HCl solution (12 M) were prepared in a separate beaker and kept between 0 and 5 ℃. The HCl/water solution was then added dropwise onto the 4,4′-oxydianiline/$NaNO_2$ mixture and stirred for about 30–45 mins. The obtained diazonium salt solution was stored at 0–5 ℃.

2.1.2. Step-2. Azo coupling reaction

1-Naphtylamine (2 mmol, 0.29 g) was dissolved in ethanol, and the mixture placed in an ice bath at a temperature between 0 and 5 °C. The previously prepared diazonium salt solution was then added dropwise to the 1-naphtylamine/ethanol solution over approximately one hour. The solution temperature was maintained between 0 and 5 °C throughout the process. After the precipitation was completed, the mixture was stirred for another 120 min at the same temperature. The solution was removed from the ice bath and stirred at room temperature for approximately 24 h. The produced precipitate was filtered and dried. The crude product was recrystallized in a 1:1 ethanol:water mixture. The crystals were first dried at room temperature and then over $CaCl_2$ in a vacuum desiccator before its characterization.

2.2. ^1H NMR, ^{13}C NMR, FTIR and ESI-MS characterization of the synthesized product

The infrared spectrum of the obtained solid compound in a KBr pellet, at room temperature, was recorded using a Perkin Elmer Spectrum 100 Fourier transform infrared (FTIR) spectrometer. Data collection was performed with 1 cm^{-1} spectral resolution and 32 scans, in the 4000–400 cm^{-1} spectral region. The ^1H and ^{13}C NMR spectra, including 2D COSY (H-H) NMR data, were obtained in DMSO-d_6 solution using a high-resolution Agilent 400 MHz NMR spectrometer. The electron

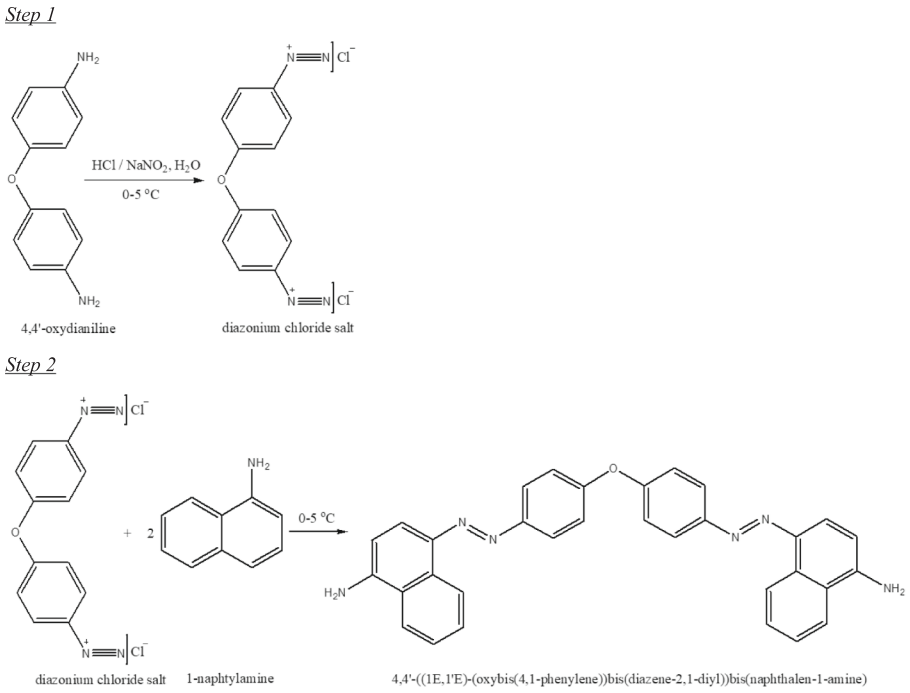

Scheme 1. Synthesis steps of 4,4′-((1*E*,1′*E*)-(oxybis(4,1-phenylene))bis(diazene-2,1-diyl))bis(naphthalen-1-amine) (**4odna**). The synthesized compound is represented in this scheme in one of the possible conformers of its *trans* N=N azo tautomeric form.

spraying ionization (ESI) mass spectrometry data were obtained for the compound (0.1286 g) dissolved in 10 ml of methanol, using an Agilent 6400 Series Triple Quadrupole B.07.01 Machine. The solution was passed through a 0.45 μm nylon filter, followed by mass scanning in the range of 100–1000 *m/z*. The obtained FTIR, ^{1}H and ^{13}C NMR spectra, as well as the positive ionizing mass spectra of the compound, are provided in the Supporting Information (Figs. S1-S4).

All the obtained spectra are in agreement with the structure of the expected product, **4odna**, resulting from the diazo coupling reaction at the *para* position (Step-2) [48,49], the experimental ^{1}H NMR spectrum being well reproduced by simulations performed using the MestReNova 14 NMR simulation software [50]. The 2D-COSY (H-H) NMR data presented in Fig. S5 (Supporting Information) further confirm the structure of the isolated product, with the protons in vicinal positions appearing correlated, as expected.

Characterization data for **4odna**: FTIR (KBr, ν/cm^{-1}): 3403 (νNH), 3116, 2977 (νCH), 1402 (νN = N), 1195 (νC–O–C). ^{1}H NMR (400 MHz, DMSO-d_6): δ 8.74 (d, J = 8.4 Hz, 1H), 8.52 (s, 1H), 8.36 (d, J = 8.2 Hz, 1H), 7.95 (d, J = 8.6 Hz, 2H), 7.75 (t, J = 7.6 Hz, 1H), 7.59 (t, J = 7.6 Hz, 1H), 7.21 (d, J = 8.1 Hz, 2H), 7.06 (d, J = 8.8 Hz, 1H), 4.64 – 4.19 (m, 2H). ^{13}C NMR (101 MHz, DMSO-d_6): δ 156.51 (s), 156.17 (s), 135.08 (s), 131.08 (s), 128.69 (s), 126.69 (s), 125.64 (s), 124.35 (s), 124.32–124.23 (m), 123.58 (s), 121.93 (s), 121.53 (s), 120.02 (s), 119.30 (s). MS (ESI^{+}, *m/z*) $C_{32}H_{24}ON_6$: $[M+H]^+$ calcd. 509.6, found 509.2; $[M+2H]^{+2}/2$ calcd. 255.3, found 255.2.

2.3. UV–vis absorption spectra

All solvents used in the experiments are of high purity spectroscopic grade and were purchased from Sigma-Aldrich. Concentrations of **4odna** solutions were prepared as low as possible (<1.2 × 10^{-5} M) in order to avoid aggregation of the compound. The ultraviolet–visible (UV–vis) spectra were obtained in the 190–800 nm wavelength range using a Perkin-Elmer Lambda-35 UV–vis spectrometer. UV irradiation of the samples was done using a 311 nm (18 W) lamp. All measurements were performed using a quartz cell (standard cell with 1 cm × 1 cm optical path), at room temperature, and after the solutions were kept in the dark for five days after preparation. The band positions were determined using second derivative spectra which were calculated with OriginPro 8.5 [51]. The uncertainty in the UV–vis measurements is ~1 nm. Spectra analysis was performed with the program Specwin32 (version 1.72.0) [52].

3. Results and discussion

3.1. Solvatochromism of *4odna*

As seen in Fig. 1(d), in the solid state **4odna** is a black and lumpy material. Fig. 1(a-c) shows pictures of solutions of **4odna** in a series of non-polar, polar-aprotic and polar-protic solvents, respectively. Most of the solutions exhibit different intense naked-eye visible colors, ranging from light yellow to burgundy, demonstrating the solvatochromism exhibited by the compound. In hydrogen bonding acceptor (HBA) and donor (HBD) solvents, the concentration of the solute is higher due to the better solubility, and the color of the solutions is more intense than in most of the non-polar and polar-aprotic solvents (e.g., benzene, chloroform, chlorobenzene and dichloromethane, but also *n*-butyl acetate) where **4odna** is poorly soluble. All solutions of **4odna** in non-polar solvents are yellow, which is also the color observed for the solutions of the compound in HBA solvents (ethyl acetate, THF, acetone, DMF, DMSO, 1,4-dioxane, toluene and diethyl ether), where the **4odna** acts as H-bond donor, while the polar-protic (HBD) solvents (except 1-octanol) give rise to burgundy solutions. The solution of **4odna** in acetonitrile (ACN) shows also tones of burgundy.

As expected, the visible region absorption spectrum of **4odna** was found to be remarkably dependent on the nature of the solvent. Figs. 2–4 show the absorption spectra of **4odna** in the three solvent groups (non-polar, polar-aprotic and polar-protic, respectively), at room temperature (25 °C). The spectra exhibit three bands in the visible region, within the 425–448 nm (band-1), 476–511 nm (band-2) and 571–577 nm (band-3) wavelength ranges (see Table 1). Bands -1 and -2 are common to all the spectra, while band-3 is observed only in polar-protic solvents and acetonitrile.

As it can be seen in Figs. 2–4, the spectra exhibit relatively broad

Fig. 1. Solutions of **4odna** in different solvents: (a) polar-aprotic; (b) non-polar; (c), polar-protic, and (d) a sample of the solid compound. In each group, the solutions are ordered by increasing dielectric constant (ε) of the solvent.

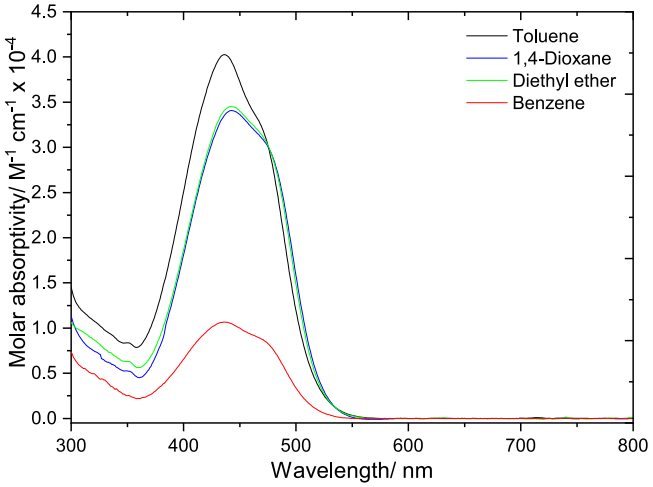

Fig. 2. UV–vis absorption spectra of **4odna** in non-polar solvents.

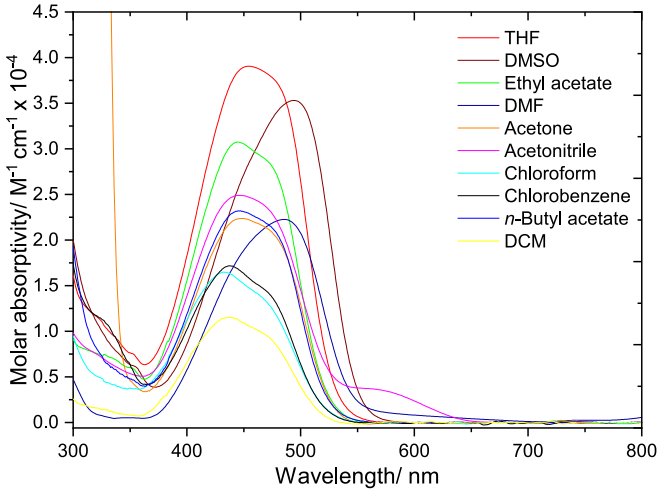

Fig. 3. UV–vis absorption spectra of **4odna** in polar-aprotic solvents.

bands. In the studied non-polar solvents (toluene, 1,4-dioxane, diethyl ether and benzene), band-1 is observed between 431 and 435 nm, and band-2 between 476 and 482 nm. For polar-aprotic solvents, band-1 has maximum within nearly the same range as in the case of non-polar solvents, 432–438 nm, except for THF (448 nm) and the two solvents

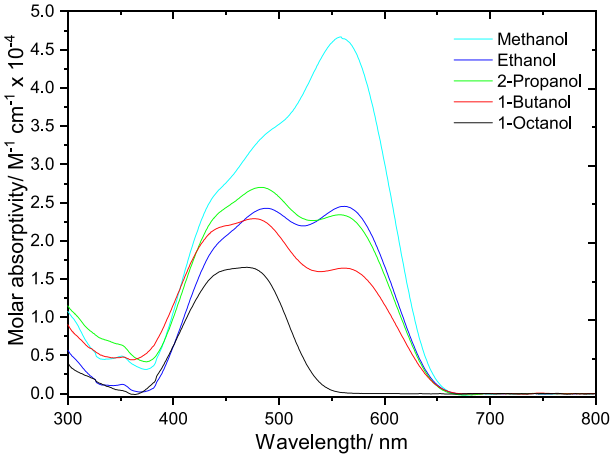

Fig. 4. UV–vis absorption spectra of **4odna** in polar-protic solvents.

with higher $E_T(30)$, DMF and DMSO, where the band appears bathochromically shifted to 446 and 448 nm, respectively. Taking as reference the shorter wavelength observed for band-1 in benzene solution (431 nm), a bathochromic shift of 17 nm is observed in the case of the most polar-aprotic solvent, DMSO.

A similar behavior is observed for band-2. In the lowest $E_T(30)$ polar-aprotic solvents band-2 has its maximum in the 477–484 nm range, which does not differ much from that observed in non-polar solvents, while in THF, DMF and DMSO solutions the band-2 maximum is observed at 492, 503 and 511 nm, respectively. In going from benzene to DMSO, band-2 undergoes a bathochromic shift of 35 nm. As seen in Fig. 1, these changes make the color of the solutions to change from matte yellow, as observed for toluene, to bright yellow in the case of DMSO, with THF and DMF solutions showing intermediate colors. Considering only the group of polar-aprotic solvents, band-1 and band-2 exhibit 23 and 34 nm bathochromic shifts, respectively, in going from chloroform (the less polar-aprotic solvent investigated) to DMSO (the most polar one). On the other hand, within the group of non-polar solvents, band-1 experiences only a minor bathochromic shift of 4 nm with the increase of $E_T(30)$ (see Table 1), with a similar bathochromic shift being observed for band-2 (6 nm, from benzene to 1,4-dioxane).

Band-3 is characteristic of polar-protic (HBD) solvents, with its maximum spreading from 571 to 577 nm, and is responsible for the burgundy tone of the solutions of **4odna** in the alcoholic solvents. The exception is 1-octanol, the alcohol having the longest aliphatic chain and the lowest $E_T(30)$, which does not seem to efficiently act as hydrogen-bond donor to **4odna**. On the other hand, band-3 is observed

Table 1
Reichardt's solvent parameter (E_T(30), kcal/mol), maximum wavelength (λ_{max}, nm) of the visible region absorption bands of **4odna**, and E_T(**4odna**) (in kcal/mol) obtained from the spectroscopic data (band-1 and band-2).

No	Solvents	E_T(30)	Band-1 λ_{max}	E_T(**4odna**)	Band-2 λ_{max}	E_T (**4odna**)	Band-3
1	toluene	33.9	435	65.7	476	60.1	
2	benzene	34.3	431	66.3	476	60.1	
3	diethyl ether	34.5	434	65.9	480	59.6	
4	1,4-dioxane	36.0	434	65.9	482	59.3	
5	chlorobenzene	36.8	432	66.2	479	59.7	
6	THF	37.4	441	64.8	492	58.1	
7	ethyl acetate	38.1	438	65.3	484	59.1	
8	*n*-butyl acetate	38.5	436	65.6	484	59.1	
9	chloroform	39.1	425	67.3	477	59.9	
10	DCM	40.7	433	66.0	477	59.9	
11	acetone	42.2	438	65.3	488	58.6	
12	DMF	43.2	446	64.1	503	56.8	
13	DMSO	45.1	448	63.8	511	56.0	
14	acetonitrile	45.6	433	66.0	484	59.1	577
15	1-octanol	48.1	436	65.6	489	58.5	
16	2-propanol	48.4	435	65.7	486	58.8	574
17	1-butanol	49.7	432	66.2	486	58.8	575
18	ethanol	51.9	434	65.9	489	58.5	573
19	methanol	55.4	428	66.8	482	59.3	571

as a weak feature in acetonitrile solution, which is formally grouped together with the polar-aprotic solvents, but does indeed possess a significant hydrogen bond donating ability (see the value of the HBD-related solvent Catalán and Kamlet-Taft parameters SA and α, respectively, shown in Table 2, for this solvent). Interestingly, band-3 shows a hypsochromic shift with the increase of E_T(30) of the solvent, from acetonitrile (577 nm) to methanol (571 nm), i.e., a shift of –6 nm.

For better understanding the solvatochromism exhibited by **4odna**, the E_T(**4odna**) values obtained from band-1 and band-2 in the different solvents were plotted against the E_T(30) values of the solvents in Fig. 5.

The plots clearly show occurrence of reversal in solvatochromism for both band-1 and band-2. Indeed, in going from the polar-protic solvent with higher E_T(30), methanol (E_T(30) = 55.4 kcal mol^{-1}) to polar-aprotic DMSO (E_T(30) = 45.1 kcal mol^{-1}), the E_T(**4odna**) values decrease from 66.8 and 59.3 kcal mol^{-1}, for band-1 and band-2, respectively, to 63.8 and 56.0 kcal.

mol^{-1}. In other words, both band-1 and band-2 undergo hypsochromic shifts with the increase of solvent polarity (negative solvatochromism). In contrast, upon changing the solvent from DMSO to non-polar toluene (E_T(30) = 33.9 kcal mol^{-1}) and benzene (E_T(30) = 34.3 kcal.

mol^{-1}), the E_T(**4odna**) values increase from 63.8 and 56.0 kcal mol^{-1} to 65.7/66.3 kcal mol^{-1} and 60.1 kcal mol^{-1}, for band-1 and band-2, respectively, i.e., as already mentioned bathochromic shifts of the bands are observed with the increase of the polarity of the solvent (positive solvatochromism). By looking to the E_T(**4odna**) values shown in Table 1, it can then be concluded that, as measured by the E_T(**4odna**) values obtained from bands -1 and -2 maxima, **4odna** exhibits a general positive solvatochromism for solvents with E_T(30) values in the ~34–45 kcal mol^{-1} range, and negative solvatochromism for solvents with E_T(30) values higher than ~45 kcal mol^{-1}, i.e., it shows a reversal in the solvatochromism at an E_T(30) value of *ca.* 45 kcal mol^{-1}, characteristic of DMSO.

3.2. *Analysis of solvatochromic behavior of **4odna** using multiparametric models*

Solvent induced spectral shifts are controlled by specific (e.g., hydrogen bonding) and nonspecific (dipolarity and polarizability effects) interactions between the solute and the solvent. In order to comprehensively evaluate the relative importance of the different intrinsic solvent parameters in determining solvent-induced spectral

Table 2
Dielectric constants, Reichardt's E_T(30) (kcal/mol), and Kamlet-Taft and Catalán solvent parameters for the used solvents [1,55,59,60].

		ε	E_T(30)	Catalán parameters				Kamlet-Taft parameters		
No	Solvent			SA	SB	SP	SdP	α (HBD)	β (HBA)	π*
1	toluene	2.38	33.9	0.000	0.128	0.782	0.284	0.00	0.11	0.54
2	benzene	2.27	34.3	0.000	0.124	0.793	0.270	0.00	0.10	0.59
3	diethyl ether	4.20	34.5	0.000	0.562	0.617	0.385	0.00	0.47	0.27
4	1,4-dioxane	2.21	36.0	0.000	0.444	0.737	0.312	0.00	0.37	0.55
5	chlorobenzene	5.62	36.8	0.000	0.182	0.833	0.537	0.00	0.07	0.71
6	THF	7.58	37.4	0.000	0.591	0.714	0.634	0.00	0.55	0.58
7	ethyl acetate	6.02	38.1	0.000	0.542	0.656	0.603	0.00	0.45	0.55
8	*n*-butyl acetate	5.07	38.5	0.000	0.525	0.674	0.535	0.00	0.45	0.46
9	chloroform	4.89	39.1	0.047	0.071	0.783	0.614	0.44	0.00	0.58
10	DCM	8.93	40.7	0.040	0.178	0.761	0.769	0.13	0.10	0.82
11	acetone	20.56	42.2	0.000	0.475	0.651	0.907	0.08	0.48	0.71
12	DMF	36.71	43.2	0.031	0.613	0.759	0.977	0.00	0.69	0.88
13	DMSO	46.45	45.1	0.072	0.647	0.830	1.000	0.00	0.76	1.00
14	acetonitrile	35.94	45.6	0.044	0.286	0.645	0.974	0.19	0.31	0.75
15	1-octanol	10.30	48.1	0.299	0.923	0.713	0.454	0.77	0.81	0.40
16	2-propanol	19.92	48.4	0.283	0.830	0.633	0.808	0.76	0.95	0.48
17	1-butanol	17.51	49.7	0.341	0.809	0.674	0.655	0.79	0.88	0.47
18	ethanol	24.55	51.9	0.400	0.658	0.633	0.783	0.83	0.77	0.54
19	methanol	32.66	55.4	0.605	0.545	0.608	0.904	0.93	0.62	0.60

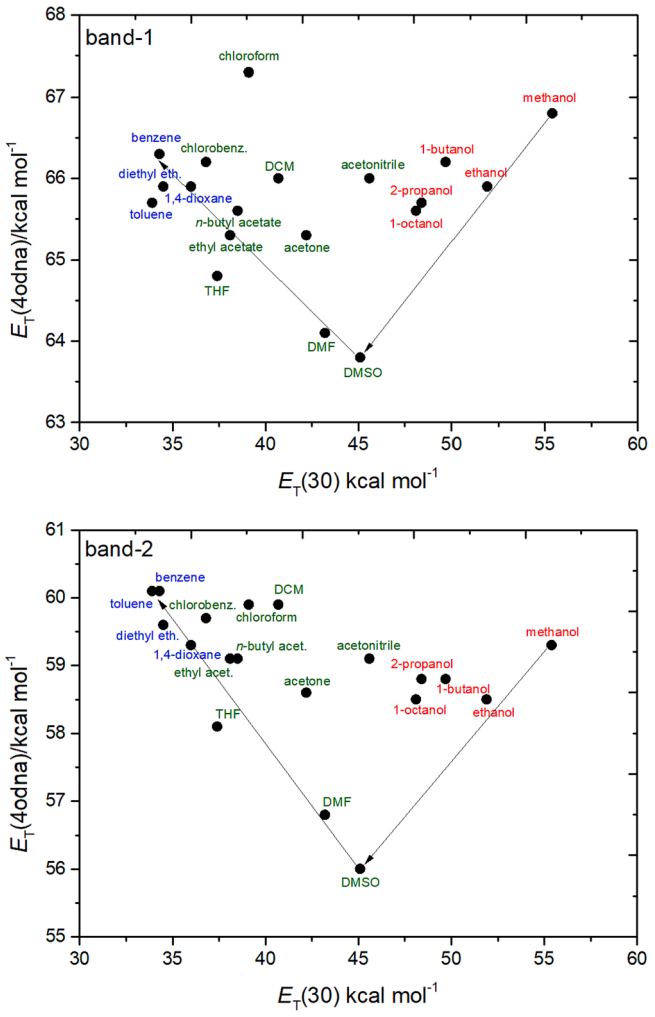

Fig. 5. Plots of E_T(4odna) values *vs.* Reichardt's E_T(30) parameters for band-1 (*top*) and band-2 (*bottom*) in various solvents. Color code: blue, non-polar solvents; green, polar-aprotic solvents; red, polar-protic solvents. (For interpretation of the references to color in this figure legend, the reader is referred to the web version of this article.)

shifts, the Kamlet-Taft and the Catalán solvatochromism methods, which are based on multiparametric empirical relations [53–58], are commonly employed.

The Kamlet-Taft and of Catalán [53–58] solvatochromic models may be formulated as in Eqs. (2) and (3), respectively:

$$E_T(\text{dye}) = E_T(\text{dye})_0 + a\alpha + b\beta + s\pi^* \quad (2)$$

$$E_T(\text{dye}) = E_T(\text{dye})_0 + a(\text{SA}) + b(\text{SB}) + d(\text{SP}) + e(\text{SdP}) \quad (3)$$

In the Kamlet-Taft model Eq. (2), α, β and π* are parameters related to the hydrogen bond donor (HBD) and hydrogen bond acceptor (HBA) capacities, and the dipolarity/polarizability of the solvent, respectively, while in the Catalán model Eq. (3) the parameters SA, SB, SP and SdP are correspondingly related with the HBD, HBA, polarizability and dipolarity of the solvent. The values of these parameters [1,55,59,60] for the solvents used in the present study are collected in Table 2 (together with dielectric constants and E_T(30) values).

In Eqs. (2) and (3), $E_T(\text{dye})_0$ is a parameter representing the E_T(dye) value for a solvent-unaffected dye, and *a*, *b*, *d*, *e* and *s* are the coefficients that reflect the contribution of the different solvent parameters to the E_T(dye) values determined from the observed band shifts in the different solvents.

In the present study, multiple linear regression analysis (MLRA) was carried out based on the obtained solvatochromic data using the Kamlet-Taft and Catalán models to determine the relative contributions of the different solvent properties to the E_T(**4odna**) values. The resulting $E_T(\text{dye})_0$ values, models' coefficients and the regression statistical quality parameters are given in Table 3. From this table it can be seen that the magnitudes of the coefficients estimated from the Catalán model vary in the order $d > a \approx b > e$ for band-1 and $d >$ b $\approx e \approx a$ for band-2, while those obtained from the Kamlet-Taft model follow the order $b > a = s$ for band-1 and $b > s > a$ for band-2. Thus, for band-1, it can be concluded that the HBD and HBA solvent parameters (affected by the *a* and *b* coefficients, respectively) have similar contributions to the measured E_T(**4odna**) values according to both Catalán and Kamlet-Taft models, though in opposite directions, the first leading to a hypsochromic wavelength shift (higher E_T(**4odna**) values) and the second to a bathochromic shift. According to the Kamlet-Taft model, the contribution of the dipolarity/polarizability (*s* parameter) is also similar in magnitude to those of *a* and *b*, and like this latter leads to a bathochromic shift. The Catalán model, where dipolarity and polarizability effects are considered in separate, reveals that polarizability (as measured by the *d* parameter) is considerably more important than dipolarity (*e* parameter). In its turn, in the case of band-2, the HBA and dipolarity/polarizability solvent parameters can be concluded to be the most effective in determining the observed spectral shifts according to both developed models.

As pointed out above, it is worth highlighting that for both bands-1 and -2, the HBD coefficient *a* is positive and the HBA coefficient *b* is negative in both Catalán and Kamlet-Taft developed solvatochromic models, indicating the energies of the transitions associated with the two bands increase when the **4odna** molecule form hydrogen bonds with the solvent as acceptor, and reduce when it acts as hydrogen bond donor, these trends being clearly noticed in the plots shown in Fig. 5, in particular when we compare the location of the cluster formed by the alcoholic solvents with the position of the more aprotic-polar hydrogen-bond acceptor solvents (like DMF and DMSO). The negative HBA coefficient *b* also justifies partially the relative position of the clusters due to polar-aprotic and non-polar solvents along the E_T(**4odna**) axis in the figure. The same general considerations apply also to band-2.

In addition, although the hydrogen bond related factors have a decisive role in determining the observed shifts in the positions of band-1 and band-2, polarizability and dipolarity effects of the solvent do also contribute considerably to this. In the Kamlet-Taft model these effects are described as a whole by the solvent parameter π*, while in the Catalán model they are described in separate by the SP and SdP terms, respectively (see Eqs. (2) and (3)). The coefficients associated with these terms (*s*, *d* and *e*) are all negative for both models both for band-1 and band-2, indicating that polarizability and dipolarity solvent effects

Table 3
$E_T(\text{dye})_0$ values and coefficients *a*, *b*, *d*, *e* and *s* obtained from the performed Catalán and Kamlet-Taft multiparametric analysis, using E_T(**4odna**) data obtained from the maximum absorption wavelengths of band-1 and band-2 observed in the studied solvents. The number of solvents (*N*), correlation coefficient (R^2) and the statistical parameters (F and P) obtained in the different fittings are also provided.

	Band-1		Band-2	
Dye analysis	Catalán	Kamlet-Taft	Catalán	Kamlet-Taft
$E_T(\text{dye})_0$	70.5 ± 1.4	67.4 ± 0.3	67.2 ± 1.7	61.1 ± 0.4
a	3.2 ± 0.7	1.9 ± 0.2	1.7 ± 0.8	0.3 ± 0.3
b	–2.8 ± 0.5	–2.6 ± 0.3	–3.5 ± 0.6	–2.2 ± 0.4
s	–	–1.5 ± 0.4	–	–1.3 ± 0.6
d	–4.1 ± 1.7	–	–7.1 ± 1.7	–
e	–1.4 ± 0.5	–	–2.6 ± 0.4	–
N	19	19	19	19
R	0.878	0.954	0.936	0.942
R^2	0.771	0.909	0.876	0.887
F	11.8	27.7	24.7	39.1
P	0.000	0.000	0.000	0.000

contribute to reduce the energy of the transitions that are associated with both bands. Accordingly, it can be seen in the plots shown in Fig. 5 that, for solvents of large polarizability and dipolarity, the E_T(**4odna**) values tend to be comparatively small.

It is also interesting to compare the positions of the solvent unperturbed bands -1 and -2 predicted by the two developed solvatochromic models, directly extracted from the obtained E_T(**4odna**)$_0$ term. For band-1, these values are 406 ± 8 and 424 ± 2 nm, as predicted by the Catalán and Kamlet-Taft models, respectively, while for band-2 they are 425 ± 11 and 468 ± 3 nm, respectively. As expected, these values are hypsochromically shifted regarding the position of the band observed in benzene and toluene (435 and 431 nm for band-1 in benzene and toluene, respectively; 476 nm for band-2 in both solvents), due to the above mentioned effects of the polarizability and dipolarity of the solvent.

Fig. S6 shows plots of the calculated E_T(**4odna**) values for band-1 and band-2 using the developed Catalán and Kamlet-Taft models as a function of the E_T(**4odna**) values obtained from the experimental data, demonstrating the good general predictive ability of both models, but letting also clear that specific solute–solvent interactions are also relevant for several of the solvents, which limit in some extent the goodness of the fits, as revealed by the R^2 values of the fittings.

3.3. Molecular interpretation of the solvatochromism in *4odna*

Structurally speaking, **4odna** is a complex system, since it may exhibit azo-hydrazone (and amine-imine) tautomerism (see Scheme 2) as well as *trans–cis* isomerism about the N=N (in the azo forms) or C=N (in the hydrazone forms) bonds, with each species possessing several conformers. On our previous study on 2-(*p*-tolyldiazenyl)naphthalen-1-amine (**2tona**) [7], which shares all these structural features with **4odna** (and does also exhibit solvatochromism), we showed that the energies of several of the possible forms of the compound are close enough to allow for their co-existence in solution. The same can be expected to happen for **4odna**.

Noteworthy, the absorption spectrum of **2tona** in the visible region is rather similar to that of **4odna**, with three bands observed within the 420–451, 445–482 nm and 548–568 nm wavelength ranges. These bands have parallel with band-1, band-2 and band-3 in the spectrum of **4odna**, and, as it happens for band-3 of **4odna**, the longest wavelength of the UV spectrum of **2tona** is only observed in solvents with significant HBD ability [7]. The two bands appearing at shortest wavelengths in the UV spectrum of **2tona** were assigned in our previous study, with help of a series of extensive time dependent density functional theory (TD-DFT) calculations, to different conformers of the *trans* N=N azo tautomer of the compound, which was found to be present in all solutions studied in significant amounts, while the band observed at the longest wavelength was ascribed to the hydrazone tautomeric form, which exists in significant amounts only in solvents with high HBD ability [7]. Though **4odna** is a structurally more complex molecule than **2tona**, due to its double azo-hydrazone and amine-imine tautomerisms and larger number of *cis/trans* isomeric forms as well as conformers, similar assignments can be safely proposed for the three bands appearing in the visible range of the absorption spectra of the two compounds. Hence, bands-1 and -2 of **4odna** can be attributed to different conformers of the azo forms of the compound, which are then present in all solutions studied in significant amounts, and band-3 to hydrazone tautomeric forms of the compound, which shall only exist in significant amounts in solvents with high HBD ability that mediate their equilibrium with the azo forms [7]. As shown in Section 3.2, band-1 is more sensitive to the HBD capacity of the solvent than band-2, implying that band-1 receives predominant contributions from conformers of the azo tautomeric form of **4odna** where both the azo and amino groups are more exposed to the solvent (i.e., more open structures) to participate in the hydrogen bonding as acceptors. According to the relative intensities of band-1 and band-2 in the spectra of **4odna** in non-polar or weakly polar solvents (see Figs. 2 and 3), with band-1 being more intense than band-2, it can also be concluded that these more open conformers of the azo tautomeric form are preferred in this type of solvents, and, then, should have a lower dipole moment than the structurally more closed forms contributing to band-2 and becoming more populated in the more polar solvents.

3.4. Photochromism of *4odna* in different solvents upon irradiation at λ = 311 nm

Photochromism of **4odna** upon irradiation at $\lambda = 311$ nm, at 25 °C, was investigated in the polar-protic solvents methanol and ethanol, whose solutions are burgundy before irradiation, and in the polar-aprotic solvents dichloromethane, chloroform, chlorobenzene and acetone, whose solutions are yellow.

Upon irradiation at $\lambda = 311$ nm for 30 min, the colors of methanol and ethanol solutions were observed to change from burgundy to red and orange, respectively. The recorded absorbance spectra as a function of the irradiation time are shown in Fig. 6a-b, together with photographs of the solutions at the indicated times of irradiation. The behavior observed for these two solutions was similar: during the first ~20 min of irradiation band-3 reduced of intensity, while bands-1 and -2 became more intense. Irradiation for more than ~20 min led to the diminishment of the intensity of all the bands, the intensity reduction being very minor in the case of the ethanol solution and more pronounced in the case of the methanol solution. These observations indicate that irradiation promoted the solvent-assisted excited-state proton transfer resulting into conversion of the initially existent hydrazone forms of the compound into its azo forms and also that for long irradiation times the compound starts to photodegrade into species with no absorption bands in the visible region. Upon subsequent storage of the irradiated solutions in the dark, the color of the solutions returned to nearly the original tone in a couple of hours, testifying occurrence of ground-state slow thermal proton transfer to reestablish the initial equilibrium between the two tautomeric forms.

In the polar-aprotic chlorinated solvents, dichloromethane (DCM), chloroform and chlorobenzene, UV irradiation promotes the change of color of the solutions from yellow to purple (Fig. 6c-e). As seen from the obtained spectra, upon irradiation bands -1 and -2 (which are due to the azo forms of **4odna**) quickly decreased of intensity, with a rate that increases from DCM to chloroform to chlorobenzene (i.e., with the decrease of the polarity of the solvent). While bands -1 and -2 were decreasing of intensity, band-3 started to be observed, together with a

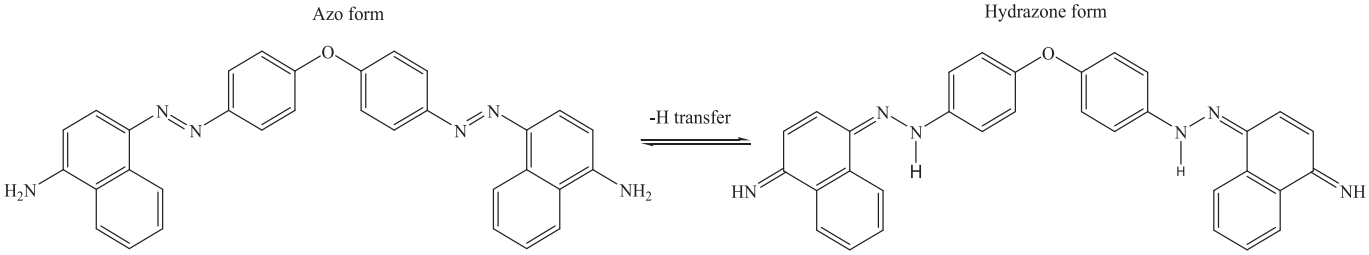

Scheme 2. Azo-hydrazone tautomerism of **4odna**. As seen in the scheme, the tautomerism also implies amine-imine tautomerism.

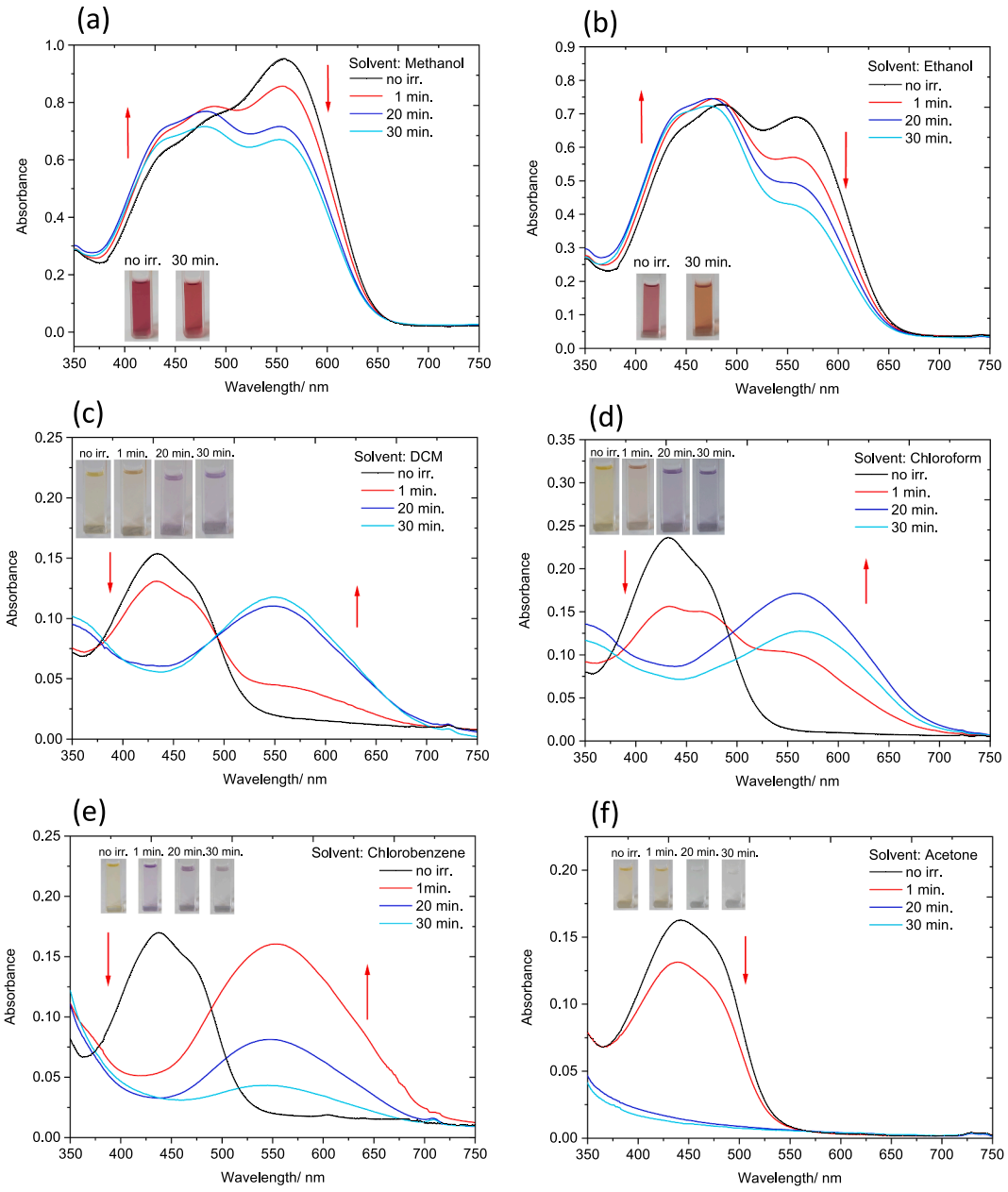

Fig. 6. Absorbance spectra of **4odna** in methanol (a), ethanol (b), DCM (c), chloroform (d), chlorobenzene (e) and acetone (f) solutions as a function of UV (λ = 311 nm) irradiation time.

new band, which appear at longer wavelengths ($\lambda_{max} \approx$ 635 nm) and overlapped with band-3. The appearance of this new band (band-4) can be attributed to the photoisomerization of **4odna** to azo and/or hydrazone higher-energy geometric isomers differing from the originally existing ones in the arrangement around the double bonds (N=N in the azo forms, and C=N in the hydrazone forms), in a similar way to what was observed before for **2tona** [7]. However, due to the structural complexity of **4odna**, the exact nature of these species could not be identified.

Very interestingly, in these solvents, a faster rate of transformation of the **4odna** azo forms initially present in solution into other species was also accompanied by a more extensive photodegradation to products with no bands in the visible region of the spectra: in DCM, until 30 min of irradiation photodegradation was negligible (with bands -3 and -4 continuously growing until this time of irradiation; Fig. 6c), while it was clearly noticeable in chloroform (where bands -3 and -4 grew during the first ~20 min of irradiation and then started to decrease; Fig. 6d), and is dominant in chlorobenzene, where it started to be observed to take place extensively after the very first minutes of irradiation (the intensity of bands -3 and -4 reached their maximum at ~1 min of irradiation; Fig. 6e). The photodegradation of **4odna** is easily observed at naked-eye due to discoloration of the sample (see Fig. 6).

Subsequent experiments in the studied polar-aprotic chlorinated solvents were also made using shorter irradiation times, after which the solutions were kept in the dark in order to check for occurrence of thermal back reactions. These experiments revealed that such processes did not take place, the solutions keeping the colors they got after irradiation.

The results of the irradiation experiments performed for **4odna** in acetone solution were unique. In this case, the initially present azo forms, responsible for the yellow color of the solution, undergo fast photodegradation to species that do not absorb in the visible spectral region, leading to prompt discoloration of the sample (Fig. 6f). Noteworthy, the hydrazone tautomer of **4odna** was not produced in this case.

Besides the points addressed above, the structural complexity of the system precludes further discussion of the mechanistic details and additional reasons for the specific different photochromic behavior of **4odna** in the different solvents. These questions thus stay as open questions for future investigations.

3.5. *Thermochromism of **4odna***

Thermochromism of **4odna** was investigated in ethanol and chlorobenzene. In ethanol, increasing the temperature from room temperature (25 °C) to 65 °C led to an increase of the intensity of both band-1 and band-2 and a decrease of band-3, which indicate ground state conversion of the hydrazone forms of the compound into the azo forms, accompanied by the concomitant color change from burgundy to orange (Fig. 7a). The changes were found to be reversible, with the solution promptly (a few minutes) returning to the original color upon lowering the temperature to room temperature. These results demonstrate the temperature dependence of the equilibrium between the ground state azo and hydrazone forms of **4odna** in ethanol, and also that the azo forms have a net higher energy than the hydrazone forms in this solvent. On the other hand, in chlorobenzene, heating the solution from room temperature up to 115 °C did not change the yellow color of the solution due to the azo forms of **4odna**, though the spectra were noticed to globally increase of intensity with temperature, revealing the temperature dependence of the absorptivity of bands -1 and -2 (Fig. 7b). Interestingly, at 115 °C the yellow colored solution became orange during the recording of the UV–vis spectrum, which was in fact noticed to differ strongly from the original spectrum, in particular because it presents the characteristic longer wavelength maxima of bands -3 and -4 of the hydrazone forms and azo/hydrazone geometric isomers of **4odna**, respectively (see Fig. 7b). This result revealed that, when exposed to the broadband UV light of the spectrometer, the azo forms of the compound initially present in solution undergo easy photo-transformation into the hydrazone forms and their higher-energy geometric isomeric forms at 115 °C, a phenomenon that was not observed to take place at lower temperatures.

4. Conclusıon

A novel bis-azo dye was synthesized and its solvatochromism was investigated in 19 solvents with different characteristics (non-polar, polar-aprotic and polar-protic). The solvatochromism exhibited by the compound was largely determined by the presence in solution of different azo or/and hydrazone forms, the latter being stabilized in solvents with strong hydrogen bond donating capacity and being responsible by the burgundy color of the solutions (in contrast to the remaining solutions that are yellow). Nevertheless, solvent effects are also relevant to change the spectral properties of the different forms of **4odna**, in particular in the case of the azo forms, whose characteristic bands (band-1 and band-2) were shown to exhibit considerable shifts with the solvent properties. For this forms, both positive and negative solvatochromism was observed, with the reversal occurring for solvents with $E_T(30)$ ~45 kcal mol^{-1}, while the hydrazone tautomer shows negative solvatochromism, with the characteristic band of this species (band-3) experiencing a hypsochromic shift with the increase of the polarity of the solvent.

The solvatochromic data were evaluated using both Catalán and Kamlet-Taft models, which demonstrate that **4odna** spectral profile displays strong sensitivity to the HBD and HBA abilities of solvent, but also a relevant dependence on solvent's dipolarity and (mostly) polarizability. The models provide also an explanation for the observed reversal in the solvatochromism exhibited by the azo forms of the compound, and also on relevant structural features of the species most contributing to band-1 and band-2, with band-1 (being more sensitive to the solvent HBD ability) receiving predominant contributions from conformers of the azo tautomeric form of **4odna** where both the azo and amino groups are more exposed to the solvent (i.e., more open structures) in order to allow for their participation in the hydrogen bonding interactions as acceptors.

The photochromism of **4odna** (induced by UV light; $\lambda = 311$ nm) was evaluated in both polar-protic (methanol and ethanol) and polar-aprotic (DCM, chloroform, chlorobenzene and acetone) solvents. Solvent-assisted excited state proton transfer was induced by the UV light, leading to conversion of the hydrazone forms of **4odna** into the azo forms, in methanol and ethanol, which thermally revert back to the initial equilibrium between these species after the solutions are let in the dark for some hours after irradiation. In the polar-aprotic chlorinated solvents (DCM, chloroform and chlorobenzene), irradiation led to irreversible photoconversion of the azo tautomeric species initially present in solution into the hydrazone forms present initially in the polar-protic solvents (e.g., methanol and ethanol) and also to the photoisomerization of **4odna** into higher-energy azo and/or hydrazone geometric isomers differing from the originally existing ones in the arrangement around the double bonds (N=N in the azo forms, and C=N in the hydrazone forms), in a similar way to what was observed before for the analogue compound **2tona** [7]. These processes, which take place at different rates in the different studied solvents (being faster in the less polar solvent), occur together with photodegradation of the compound and production of species with no absorption in the visible spectral range. In acetone solution, photodegradation is very fast, leading to prompt discoloration of the sample, with no evidence of formation of the hydrazone tautomeric species of **4odna**.

Temperature dependence of the color of the solutions of **4odna** in ethanol and chlorobenzene was also evaluated, with the compound showing reversible thermochromic behavior in the first solvent. In chlorobenzene, no thermochromism was observed, but a change of color

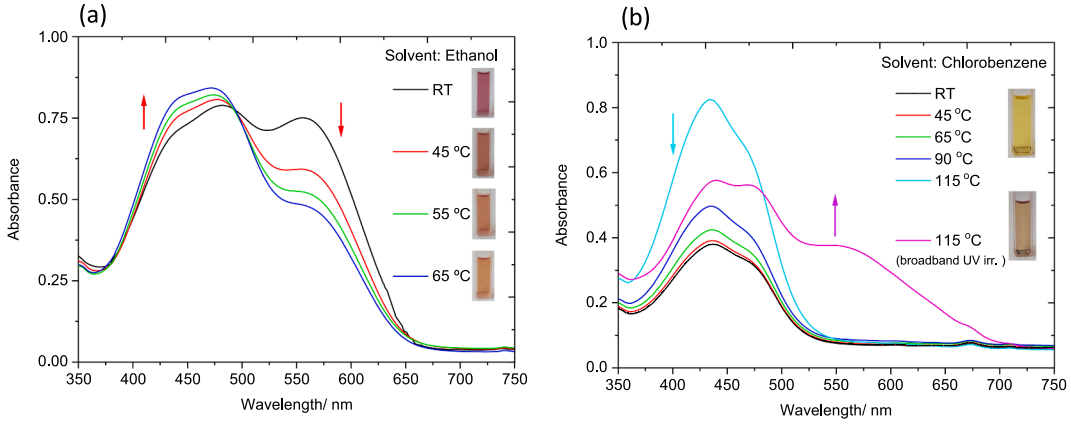

Fig. 7. Absorbance spectra of **4odna** in ethanol (a) and chlorobenzene (b) as a function of temperature.

of the solution was promptly induced by the UV–vis broadband source beam of the spectrometer when the absorbance spectrum of the solution was being recorded at $T = 115$ °C, which demonstrates that the azo forms of **4odna** undergo easy photo-transformation into the hydrazone forms in this solvent at high temperature.

CRediT authorship contribution statement

İsa Sıdır: Writing – review & editing, Writing – original draft, Validation, Methodology, Investigation, Funding acquisition, Formal analysis, Data curation. **Yunus Emre Kara:** Data curation. **Yadigar Gülseven Sıdır:** Formal analysis, Data curation, Conceptualization. **Halil Berber:** Formal analysis, Data curation. **Rui Fausto:** Writing – review & editing, Writing – original draft, Methodology, Funding acquisition, Formal analysis, Data curation, Conceptualization.

Declaration of Competing Interest

The authors declare that they have no known competing financial interests or personal relationships that could have appeared to influence the work reported in this paper.

Data availability

No data was used for the research described in the article.

Acknowledgements

The authors greatly appreciate Bitlis Eren University Research Foundation for financial support (Projects BEBAP-2013.04, BEBAP-2014.05 and BEBAP-2022.23), the Chemistry Department, Faculty of Sciences, Eskişehir Technical University, the Portuguese Science Foundation (“Fundação para a Ciência e a Tecnologia”-FCT; Projects CQC-IMS UIDB/00313/2020 and UIDP/00313/2020 - National Funds).

Appendix A. Supplementary data

Supplementary data (Figure S1 with the FTIR spectrum of **4odna**. Figure S2 with the experimental and simulated ^{1}H NMR spectra of **4odna**. Figure S3 with the experimental ^{13}C NMR spectrum of **4odna.** Figure S4, with the +ESI mass spectra of **4odna**. Figure S5 with the 2D-COSY NMR (H-H) spectrum of **4odna**. Figure S6 with Plot of calculated E_T(**4odna**) values (kcal mol^{-1}) for band-1 and band-2 using the developed Catalán and Kamlet-Taft models as a function of the E_T(**4odna**) values (kcal mol^{-1}) obtained from the experimental data.) to this article can be found online at https://doi.org/10.1016/j.jphotochem.2023.115138.

References

[1] C. Reichardt, T. Welton, Solvents and Solvent Effects in Organic Chemistry, Wiley, 2010.
[2] P. Suppan, N. Ghoneim, Solvatochromism, Royal Society of Chemistry, Cambridge, England, 1997.
[3] A. Bagno, Probing the solvation shell of organic molecules by intermolecular 1H NOESY, J. Phys. Org. Chem. 15 (12) (2002) 790–795.
[4] C. Reichardt, Solvatochromic dyes as solvent polarity indicators, Chem. Rev. 94 (8) (1994) 2319–2358.
[5] O.A. El Seoud, Understanding solvation, Pure Appl. Chem. 81 (2009) 697–707.
[6] A.R. Katritzky, D.C. Fara, H. Yang, K. Tämm, T. Tamm, M. Karelson, Quantitative measures of solvent polarity, Chem. Rev. 104 (1) (2004) 175–198.
[7] İ. Sıdır, Y.G. Sıdır, H. Berber, R. Fausto, Solvato-, thermo- and photochromism in a new diazo diaromatic dye: 2-(p-tolyldiazenyl)naphthalen-1-amine, J. Mol. Struct. 1267 (2022), 133595.
[8] K. Dimroth, C. Reichardt, T. Siepmann, F. Bohlmann, Über Pyridinium-N-phenol-betaine und ihre Verwendung zur Charakterisierung der Polarität von Lösungsmitteln, Justus Liebigs Ann. Chem. 661 (1) (1963) 1–37.
[9] M. Vidal, C. Pastenes, M.C. Rezende, C. Aliaga, M. Domínguez, The inverted solvatochromism of protonated ferrocenylethenyl-pyrimidines: the first example of the solvatochromic reversal of a hybrid organic/inorganic dye, Org. Chem. Front. 6 (2019) 3896–3901.
[10] A. Mukhopadhyay, K.J. Mandal, J.N. Moorthy, Anionic merocyanine dyes based on thiazol-2-hydrazides: reverse solvatochromism, preferential solvation and multiparametric approaches to spectral shifts, Phys. Chem. Chem. Phys. 20 (2018) 4149–4159.
[11] S. Panigrahi, S.P. Biswal, P.K. Misra, Disclosure of the solvatochromism and the reversal switch in some tailor-made electron push-push anils, J. Mol. Liq. 329 (2021), 115536.
[12] C.E.A. de Melo, L.G. Nandi, M. Domínguez, M.C. Rezende, V.G. Machado, Solvatochromic behavior of dyes with dimethylamino electron-donor and nitro electron-acceptor groups in their molecular structure, J. Phys. Org. Chem. 28 (4) (2015) 250–260.
[13] Y. Zheng, X.-X. Zhang, L. Shi, T.-B. Ren, L. Yuan, X.-B. Zhang, Reversal of solvatochromism: A new strategy to construct activatable two-photon fluorescent probes for sensing, Chem. Asian J. 17 (2022), e202101197.
[14] M.E. Gemayel, K. Börjesson, M. Herder, D.T. Duong, J.A. Hutchison, C. Ruzié, G. Schweicher, A. Salleo, Y. Geerts, S. Hecht, E. Orgiu, P. Samorì, Optically switchable transistors by simple incorporation of photochromic systems into small-molecule semiconducting matrices, Nat. Commun. 6 (1) (2015) 1–8.
[15] M. Irie, Advances in photochromic materials for optical data storage media, Jpn. J. Appl. Phys. 28 (1989) 215.
[16] M. Tomasulo, S. Sortino, F.M. Raymo, A fast and stable photochromic switch based on the opening and closing of an oxazine ring, Org. Lett. 7 (6) (2005) 1109–1112.
[17] R. Siewertsen, H. Neumann, B. Buchheim-Stehn, R. Herges, C. Näther, F. Renth, F. Temps, Highly efficient reversible Z- E photoisomerization of a bridged azobenzene with visible light through resolved S1 (nπ*) absorption bands, J. Am. Chem. Soc. 131 (43) (2009) 15594–15595.
[18] M.-M. Russew, S. Hecht, Photoswitches: from molecules to materials, Adv. Mater. 22 (2010) 3348–3360.
[19] S. Kawata, Y. Kawata, Three-dimensional optical data storage using photochromic materials, Chem. Rev. 100 (5) (2000) 1777–1788.
[20] M. Irie, Photochromism of diarylethene molecules and crystals, Proc. Jpn. Acad. Ser. B Phys. Biol. Sci. 86 (5) (2010) 472–483.
[21] J. Cusido, E. Deniz, F.M. Raymo, Fluorescent switches based on photochromic compounds, Eur. J. Org. Chem. 2009 (13) (2009) 2031–2045.
[22] H. Chen, Y. Liao, Photochromism based on reversible proton transfer, J. Photochem. Photobiol. A Chem. 300 (2015) 22–26.
[23] X. Zhang, L. Hou, P. Samorì, Coupling carbon nanomaterials with photochromic molecules for the generation of optically responsive materials, Nat. Commun. 7 (2016) 1–14.
[24] S.-J. Lim, J. Seo, S.Y. Park, Photochromic switching of excited-state intramolecular proton-transfer (ESIPT) fluorescence: a unique route to high-contrast memory switching and nondestructive readout, J. Am. Chem. Soc. 128 (2006) 14542–14547.
[25] E. Merino, M. Ribagorda, Control over molecular motion using the cis–trans photoisomerization of the azo group, Beilstein J. Org. Chem. 8 (2012) 1071–1090.
[26] H.M.D. Bandara, S.C. Burdette, Photoisomerization in different classes of azobenzene, Chem. Soc. Rev. 41 (5) (2012) 1809–1825.
[27] X. Xu, P. Zhang, B.o. Wu, Y. Xing, K.e. Shi, W. Fang, H. Yu, G. Wang, Photochromic dendrimers for photoswitched solid-to-liquid transitions and solar thermal fuels, ACS Appl. Mater. Interfaces. 12 (44) (2020) 50135–50142.
[28] S. Tan, Y.e. Sha, T. Zhu, M.A. Rahman, C. Tang, Photoresponsive supramolecular polymers based on quadruple hydrogen-bonding and a photochromic azobenzene motif, Polym. Chem. 9 (44) (2018) 5395–5401.
[29] J.-F. Yan, R.-X. Men, X.-X. Chen, C.-X. Lin, P. Nockemann, Y.-F. Yuan, D–π–A type ferrocene-substituted azobenzene photochromic switches: synthesis, structures, and electrochemical and photoisomerization studies, New J. Chem. 45 (2021) 19917–19927.
[30] C. Lin, S. Maisonneuve, C. Theulier, J. Xie, Synthesis and photochromic properties of azobenzene-derived glycomacrolactones, Eur. J. Org. Chem. 2019 (8) (2019) 1770–1777.
[31] J. Fregoni, G. Granucci, E. Coccia, M. Persico, S. Corni, Manipulating azobenzene photoisomerization through strong light–molecule coupling, Nat. Commun. 9 (2018) 1–9.
[32] Y. Yu, T. Ikeda, Alignment modulation of azobenzene-containing liquid crystal systems by photochemical reactions, J Photochem Photobiol C: Photochem Rev 5 (3) (2004) 247–265.
[33] P. Lentes, E. Stadler, F. Röhricht, A. Brahms, J. Gröbner, F.D. Sönnichsen, G. Gescheidt, R. Herges, Nitrogen bridged diazocines: Photochromes switching within the near-infrared region with high quantum yields in organic solvents and in water, J. Am. Chem. Soc. 141 (2019) 13592–13600.
[34] M. Poutanen, Z. Ahmed, L. Rautkari, O. Ikkala, A. Priimagi, Thermal isomerization of hydroxyazobenzenes as a platform for vapor sensing, ACS Macro Lett. 7 (3) (2018) 381–386.
[35] S.K. Yesodha, C.K. Sadashiva Pillai, N. Tsutsumi, Stable polymeric materials for nonlinear optics: a review based on azobenzene systems, Prog. Polym. Sci. 29 (1) (2004) 45–74.
[36] F. Aleotti, A. Nenov, L. Salvigni, M. Bonfanti, M.M. El-Tahawy, A. Giunchi, M. Gentile, C. Spallacci, A. Ventimiglia, G. Cirillo, L. Montali, S. Scurti, M. Garavelli, I. Conti, Spectral tuning and photoisomerization efficiency in push-pull azobenzenes: designing principles, J. Phys. Chem. A. 124 (46) (2020) 9513–9523.
[37] K. Rustler, P. Nitschke, S. Zahnbrecher, J. Zach, S. Crespi, B. Konig, Photochromic evaluation of 3 (5)-arylazo-1 h-pyrazoles, J. Org. Chem. 85 (2020) 4079–4088.
[38] P.F. Gordon, P. Gregory, Organic Chemistry in Colour, Springer-Verlag, Berlin, Heidelberg, New York, 1983.

[39] H. Dürr, H. Bouas-Laurenet (Eds.), Photochromism: Molecules and Systems, Elsevier, Amsterdam, 1990.
[40] P. Gregory, High-Technology Applications of Organic Colorants, Kluwer Academic Publishers, New York, 1991.
[41] F.L. Carter, A. Schultz, D. Duckworth, in: Molecular Electronic Devices II, Marcel Decker, New York, 1987, p. 183.
[42] W.M. Fabian, L. Antonov, D. Nedeltcheva, F.S. Kamounah, P.J. Taylor, Tautomerism in hydroxynaphthaldehyde anils and azo analogues: a combined experimental and computational study, Chem. Eur. J. 108 (2004) 7603–7612.
[43] H. Joshi, F.S. Kamounah, G. van der Zwan, C. Gooijer, L. Antonov, Temperature dependent absorption spectroscopy of some tautomeric azo dyes and Schiff bases, J. Chem. Soc., Perkin Trans. 2 (2001) 2303–2308.
[44] S.t. Stoyanov, L. Antonov, Quantitative analysis of azo-quinonehydrazone tautomeric equilibrium, Dyes Pigm. 10 (1) (1989) 33–45.
[45] S. Stoyanov, L. Antonov, B. Soloveytchik, V. Petrova, Quantitative analysis of tautomeric equilibrium in 1-phenylazo-4-naphthols—a new approach, Dyes Pigm. 26 (2) (1994) 149–158.
[46] H. Joshia, F.S. Kamounahb, C. Gooijera, G. van der Zwana, L. Antonovc, Excited state intramolecular proton transfer in some tautomeric azo dyes and schiff bases containing an intramolecular hydrogen bond, J. Photochem. Photobiol. A Chem. 152 (2002) 183–191.
[47] L. Antonov, S. Stoyanov, T. Stoyanova, Tautomeric equilibrium in 1-phenylazo-2-naphthol—A quantitative study, Dyes Pigm. 27 (1995) 133–142.
[48] K. Hunger, Azo Dyes, in Ullmann's Encyclopidia of Industrial Chemistry, Wiley-VCH, Einheim, 20 0 0 Chap. 1, pp. 8,9.
[49] H.S. Turner, 482. The formation of isomeric azo-compounds in the coupling of diazonium salts with 1-naphthylamine, J. Chem. Soc. (Resumed) (1949) 2282–2289.
[50] Willcott, M. MestRe Nova, Mestrelab Research S.L. Feliciano Barrera 9B, Bajo, 15706 Santiago de Compostela, Spain. Http://Www.Mestrelab.Com. See Web Site for Pricing Information, J. Am. Chem. Soc. 131 (2009)13180–13180.
[51] Origin(Pro)Version 8.5. OriginLab Corporation, 2022 Northampton, MA, USA.
[52] Spekwin32 (version 1.72), Spectroscopy Software, (not available anymore for download; replaced by Spectragryph; see https://www.effemm2.de/spekwin/index_en.html.
[53] M. El-Sayed, H. Müller, G. Rheinwald, H. Lang, S. Spange, Solvatochromism, crystallochromism, and solid state structures of hydrophilically functionalized aromatic amino ketones containing furan and thiophene rings, Chem. Mater. 15 (3) (2003) 746–754.
[54] C.T. Martins, M.S. Lima, O.A. El Seoud, Thermosolvatochromism of merocyanine polarity indicators in pure and aqueous solvents: relevance of solvent lipophilicity, J. Org. Chem. 71 (2006) 9068–9079.
[55] J. Catalán, Toward a generalized treatment of the solvent effect based on four empirical scales: dipolarity (SdP, a new scale), polarizability (SP), acidity (SA), and basicity (SB) of the medium, J. Phys. Chem. B 113 (2009) 5951–5960.
[56] A. Filarowski, M. Kluba, K. Cieślik-Boczula, A. Koll, A. Kochel, L. Pandey, W.M. De Borggraeve, M. Van der Auweraer, J. Catalán, N. Boens, Generalized solvent scales as a tool for investigating solvent dependence of spectroscopic and kinetic parameters. Application to fluorescent BODIPY dyes, Photochem. Photobiol. Sci. 9 (7) (2010) 996–1008.
[57] N. Friebe, K. Schreiter, J. Kübel, B. Dietzek, N. Moszner, P. Burtscher, A. Oehlke, S. Spange, Fluorosolvatochromism of furanyl-and thiophenyl-substituted acetophenones, New J. Chem. 39 (7) (2015) 5171–5179.
[58] A. Schade, K. Schreiter, T. Rüffer, H. Lang, S. Spange, Interactions of enolizable barbiturate dyes, Chem. Eur. J.. 22 (16) (2016) 5734–5748.
[59] M.J. Kamlet, J.L.M. Abboud, M.H. Abraham, R.W. Taft, Linear solvation energy relationships. 23. A comprehensive collection of the solvatochromic parameters, pi.*, alpha., and. beta., and some methods for simplifying the generalized solvatochromic equation, J. Org. Chem. 48 (17) (1983) 2877–2887.
[60] Y. Marcus, The properties of organic liquids that are relevant to their use as solvating solvents, Chem. Soc. Rev. 22 (1993) 409–416.